ACS Macro Letters

Letter

pubs.acs.org/macroletters

Linear Viscoelastic and Dielectric Properties of Phosphonium Siloxane Ionomers

Quan Chen,[†] Siwei Liang,[†,§] Huai-suen Shiau,[‡] and Ralph H. Colby*,[†]

[†]Department of Materials Science and Engineering and [‡]Department of Chemical Engineering, The Pennsylvania State University, University Park, Pennsylvania 16802, United States

Supporting Information

ABSTRACT: The linear viscoelastic (LVE) and dielectric relaxation spectroscopic (DRS) properties of polysiloxanes with phosphonium (fraction f) and oligo(ethylene oxide) (fraction $1-f$) side groups with a fraction of ionic monomers $f = 0-0.26$ have been studied. LVE master curves of those ionomers have been constructed. The ionic dissociation has been witnessed as a delayed polymer relaxation in LVE with increasing ion content, as well as an α_2 ionic segmental relaxation process in DRS. LVE exhibits glassy and delayed rubbery relaxation at low ionic fraction $f \leq 11\%$, where the ionic dissociation time detected in DRS enables description of LVE with a sticky Rouse model. In contrast, the glassy and rubbery stress relaxation moduli merge into one broad process at high $f \geq 22\%$, where the whole LVE response from glassy to terminal relaxation can be described phenomenologically by a single Kohlrausch–Williams–Watts (KWW) equation with the lowest stretching exponent $\beta = 0.10$ ever seen for polymeric liquids, describing LVE over 15 decades of frequency.

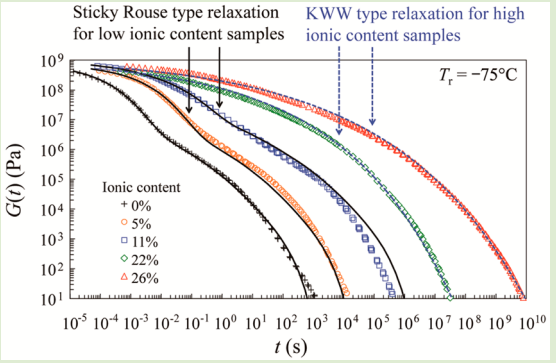

Ionomers usually contain a small percentage of ionic groups (less than 15 mol %) distributed along their backbones.[1] Ionomers have been known to have some characteristics of "thermoplastic elastomers" due to the thermally reversible networks formed by associations of the ionic groups.[1−8] Dynamics of ionomers with anionic groups covalently bonded to the polymer backbone (polyanions), such as sulfonate and carboxylate, have been extensively studied in the last four decades,[1−8] where an increase of ion content leads to structural changes, e.g., microscopic ion aggregation as suggested from X-ray scattering measurements.[1,4,8] As a result, ionomers exhibit different dynamic responses compared to their nonionic counterparts, e.g., delayed terminal relaxation, two distinct T_g's, appearance of a second rubbery plateau, and pronounced viscoelasticity attributed to the long-lived ionic associations serving as thermally reversible cross-links.[1−7,9,10]

Ionomers with cationic groups (e.g., ammonium,[11] quaternized pyridine,[12] imidazolium,[13] and phosphonium[14]) attached to the backbone (polycations) are of particular interest recently owing to their potential applications such as water purification, antimicrobial agents, alkaline fuel cell membranes, and ionic actuators. It is well accepted that they have structural and dynamic features similar to polyanions. In our previous study, a group of novel polysiloxane-based ionomers grafted with oligo(ethylene oxide) (EO) and a phosphonium ionic group were synthesized via hydrosilylation reaction.[15] The physical properties, morphology, and dielectric conductivity of those phosphonium ionomers suggest (1) the interaction between a bulky phosphonium cation and its counterion is so weak that ionic pairs do not aggregate strongly and (2) the ionic interaction between the ion pair and polymer medium is weak; together these make T_g insensitive to ionic content. This study focuses on dynamic aspects of these phosphonium ionomers with the purpose of elucidating how the bulky cation and high ionic content influence the linear viscoelasticity (LVE).

LVE measurements were made with an Advanced Rheometric Expansion System (ARES, Rheometric Scientific) on the phosphonium ionomers with bromide (Br) as a counterion, having molar fraction of ionic monomers $f = 5\%$, 11%, 22%, and 26%, and their neutral counterpart ($f = 0\%$); the chemical structure is shown in Scheme 1.

Figure 1(a) shows master curves of storage and loss moduli, $G'(\omega)$ and $G''(\omega)$, measured as functions of angular frequency

Scheme 1. Chemical Structure of Phosphonium Random Copolymer Ionomers

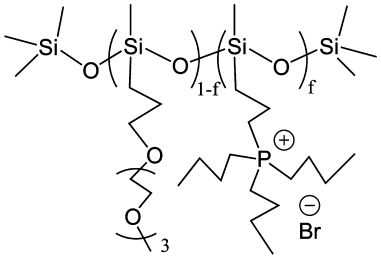

Received: September 17, 2013
Accepted: October 11, 2013
Published: October 15, 2013

   dx.doi.org/10.1021/mz400476w | *ACS Macro Lett.* 2013, 2, 970−974

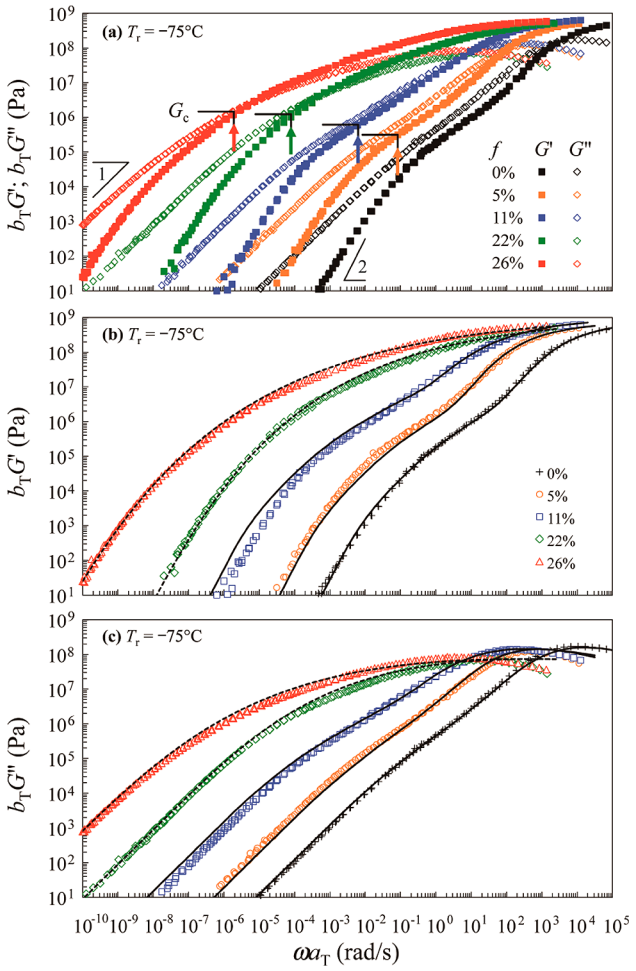

Figure 1. Master curves of storage and loss moduli, $G'(\omega)$ and $G''(\omega)$, as functions of angular frequency ω for phosphonium ionomers with different ionic fraction (from right to left f = 0%, 5%, 11%, 22%, 26% at reference temperature T_r = −75 °C). The solid curves represent theoretical fitting (eq 2) combining a glassy modulus fitted to a KWW equation and a rubbery modulus fitted to a sticky Rouse model. The dashed curves for f = 22% and 26% represent fitting the entire LVE response to a KWW equation.

ω for the samples at reference T_r = −75 °C, which is close to (within ±10 °C) their DSC T_g (cf. Table 1). It is surprising to observe (1) no clear plateau associated with ionic association and (2) that time−temperature superposition (tTs) works well for all the samples from their glassy modulus of $G_g \sim 10^9$Pa to terminal tails $G'(\omega) \propto \omega^2$ and $G''(\omega) \propto \omega$ covering a wide frequency window. Both features suggest that the ionic association is weak, in accordance with the bulky phosphonium side group and specific ion solvating ability of the EO side group: The bulky ionic group should result in steric hindrance for ionic association, and the EO group facilitates dissociation of ionic pairs. Then, the ionic association as an extra friction source is not sufficient to lead to either a plateau or failure of tTs. This argument is supported by the lack of ionic aggregation in X-ray scattering and the DSC T_g having a very weak increase with ionic content.[15]

The LVE response is quite different for samples of $f \leq 11\%$ showing distinct glassy and polymeric relaxations from those of $f \geq 22\%$, for which the glassy and rubbery relaxations are so broad that they merge into a single extremely broad process. To our best knowledge, this merging has not been reported in LVE of other ionomers.

In our previous study, we found that the LVE and dielectric relaxation spectroscopy (DRS) provide independent measures of the association lifetime τ_s that compare well:[16] For LVE, we determine the ionic dissociation frequency ω_c where the storage modulus equals to kT per ionic group, that is, $G'(\omega_c) = P_0kT$ with P_0, k, and T being number density of ionic groups, Boltzmann constant, and absolute temperature, respectively. ω_c thus-obtained at T_r (see arrows in Figure 1(a)) is extended to other T via the viscoelastic shift factors. The extended ω_c is plotted against $1000/T$ in Figure 2(a). For DRS, we first express the derivative formalism as $\varepsilon_{der} = (-\pi/2)d\varepsilon'/d \ln \omega$, where ε' is the dynamic dielectric constant.[17] ε_{der} data of all ionomer samples show three processes, the α process corresponding to segmental motion at high ω, the α_2 process corresponding to ionic dissociation at medium ω, and the electrode polarization at low ω.[16] We analyzed ε_{der} through fitting the former two processes to proper Havriliak−Negami equations and the latter process to a power law equation (see Figure S1, Supporting Information, which clearly shows the ionic α_2 process increasing in strength and broadening as ion content increases).[16,18] The frequency of dielectric maximal loss ω_{max} obtained for the α_2 process from this analysis is plotted against $1000/T$ in Figure 2(b).[18] The plots of direct current (DC) conductivity σ_{DC} against $1000/T$ are added in Figure 2(c) for testing a correlation between ionic dissociation and ion conduction as explained later. The curves in Figure 2 are the Vogel-Fulcher-Tammann (VFT) fittings.

$$\omega = \omega_0 \exp[-DT_0/(T - T_0)] \quad (1)$$

where ω_0 is the attempt frequency; T_0 is the Vogel temperature; and D is the so-called strength parameter (the fitting parameters are summarized in Table S1, Supporting Information).

In Figure 2, ω_c and ω_{max} show similar values at all temperatures. To show their correlation, ω_{max} is plotted against ω_c in Figure 3(a). These data are close to the solid line corresponding to $\omega_c = \omega_{max}$ within experimental uncertainty. A similar correlation has been noted previously for a PEO-based

Table 1. DSC Glass Transition Temperature T_g, Number Density of Ionic Groups P_0, and Fitting Parameters Utilized in Fittings of a Sticky Rouse Model and KWW Equation at T_r = −75 °C

			glassy			rubbery			
f (%)	P_0 (nm^{-3})	T_g (K)	β	τ_{KWW} (s)	$G_g(0)$ (GPa)	M_0 (Da)	τ_0 (s)	M_s (Da)	τ_s (s)
0	-	189	0.35	4.2×10^{-5}	0.81	300	3.7×10^{-3}	-	-
5	0.12	198	0.35	7.9×10^{-4}	0.73	300	5.6×10^{-2}	5400	18
11	0.23	199	0.25	1.6×10^{-3}	1.0	300	5.0×10^{0}	2500	350
22	0.44	199	0.12	1.0×10^{-3}	1.1	-	-	-	-
26	0.53	204	0.10	1.8×10^{-3}	1.3	-	-	-	-

dx.doi.org/10.1021/mz400476w | ACS Macro Lett. 2013, 2, 970−974

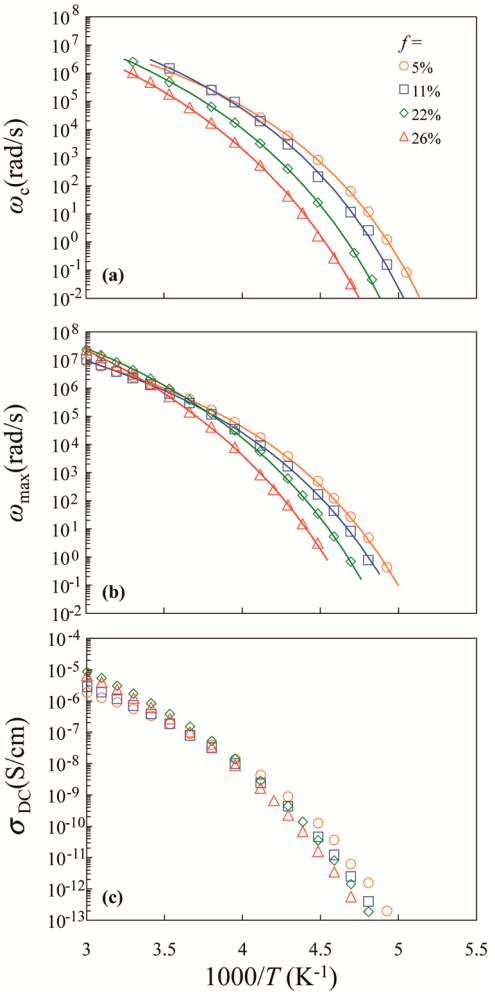

Figure 2. Temperature dependences of (a) LVE ω_c corresponding to kT per ionic group, (b) DRS peak frequency ω_{max} of the α_2 relaxation, and (c) DC conductivity. Curves are fits to the VFT equation (eq 1).

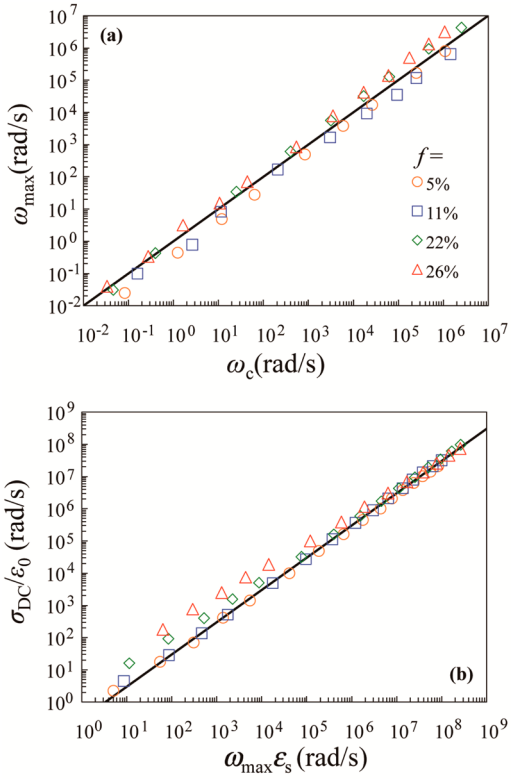

Figure 3. (a) Correlation between DRS ω_{max} and LVE ω_c, with the line corresponding to $\omega_{max} = \omega_c$. (b) Test of the BNN equation: plots of $\sigma_{DC}/\varepsilon_0$ against $\omega_{max}\varepsilon_s$, with the line corresponding to eq 4 with B = 0.3.

polyanion with Na counterion.[16] The strong correlation between ω_c and ω_{max} confirms that LVE and DRS as independent measurements detect the same ionic dissociation process.

For samples having f = 5% and 11% where both glassy and rubbery relaxations can be clearly observed, we attempt to describe the relaxation modulus $G(t)$, transferred from $G'(\omega)$ and $G''(\omega)$ in frequency domain, through a combination of the Kohlrausch–Williams–Watts (KWW) equation at high frequency (short time glassy modes) and a sticky Rouse model at lower frequency (long time polymer modes) describing the glassy and rubbery moduli, $G_g(t)$ and $G_r(t)$, respectively,[19−21]

$$G(t) = G_g(t) + G_r(t) \tag{2a}$$

$$G_g(t) = G_g(0)\exp[-(t/\tau_{KWW})^{\beta}] \tag{2b}$$

$$G_r(t) = \sum_i \frac{\rho w_i RT}{M_i}\{\sum_{p=N_{s,i}+1}^{N_i} \exp(-tp^2/\tau_0 N_i^2) + \sum_{p=1}^{N_{s,i}} \exp(-tp^2/\tau_s N_{s,i}^2)\} \tag{2c}$$

Here, $G_g(0)$, τ_{KWW}, and β are KWW fitting parameters for the glassy modulus. $G_g(0)$ is the glassy modulus for $t \to 0$; β is a shape parameter characterizing the relaxation mode distribution (smaller β means stronger stretched exponential and accordingly broader relaxation mode distribution); ρ is the density; and R is the gas constant. The weight fraction w_i of the i-th component having the molecular weight M_i was determined for the nonionic counterpart via gel permeation chromatography (GPC) with tetrahydrofuran (THF) as eluent solvent and columns calibrated using standard monodisperse polystyrene (inset of Figure S2, Supporting Information). For ionomers, the molecular weight of the i-th component is slightly larger than that of the nonionic counterpart because the monomer incorporating the cationic phosphonium group has molecular weight m_{ionic} larger than $m_{nonionic}$ of the monomer incorporating the nonionic EO side group. Then, we can use $M_i^{ionic} = M_i^{nonionic}(1 - f + fr_M)$ to represent the molecular weight of the i-th component of the ionomer samples, where $r_M = m_{ionic}/m_{nonionic}$. $N_i = M_i/M_0$ and $N_{s,i} = M_i/M_s$ are the number of Rouse and sticky Rouse segments over an i-th chain, where M_0 and M_s ($=m_{nonionic}(1-f)/f + m_{ionic}$) are the molecular weight of a Rouse and a sticky Rouse segment, respectively. For the nonionic counterpart, there is no sticky Rouse mode, allowing us to chose $N_{s,i} = 0$. We further chose M_0 = 300 according to the amplitude of a modulus where a deviation of $G(t)$ from the KWW fit of $G_g(t)$ (eq 2b) is observed, leaving τ_0 as the only fitting parameter in eq 2c. For f = 5% and 11%, we also choose M_0 = 300 by following the nonionic sample. More importantly, the ionic dissociation can be detected independently in DRS, allowing us to utilize $\tau_s = 1/\omega_{max}$ in eq 2c. The Rouse model further allows us to approximate $\tau_0 = \tau_s(M_0/M_s)^2$. This feature

dx.doi.org/10.1021/mz400476w | ACS Macro Lett. 2013, 2, 970−974

for PEO-containing polymer was attributed previously to specific ion dissolving ability of EO.[16] Strictly speaking, there is *no free adjustable parameter* in our fitting of the rubbery modulus (eq 2c). All parameters utilized in this sticky Rouse model are summarized in Table 1. $G(t)$ obtained from the fitting explained above is transferred into the frequency domain and shown as solid curves in Figures 1(b) and (c), which agree reasonably well with the experimental results, confirming the validity of the molecular picture taken in the sticky Rouse model; i.e., the ionic association serves as a sticker whose lifetime governs the slow relaxation from ionic dissociation to terminal relaxation, making these ionomers viscoelastic liquids. For samples having f = 22% and 26%, the polymer relaxations are no longer apparent. In this case, it is unreasonable to utilize the sticky Rouse model assuming separate glassy and rubbery relaxations. Here, we attempt to fit the data directly to the KWW equation, as shown in the dashed curves in Figures 1(b) and (c), with parameters summarized in Table 1. It is surprising that *all modes relax by cooperative motion for these short and high-ion-content (f = 22% and 26%) ionomer chains,* and thus a single KWW equation can describe the entire LVE master curve from glassy to terminal relaxation. In general, the stretching β is in a range of $0.5 < \beta < 0.8$ for small molecules and $0.2 < \beta < 0.6$ for polymeric liquids. The extremely low stretching exponents β = 0.1 for f = 26% and β = 0.12 for f = 22% are the lowest β values ever reported in any polymeric liquid! This result suggests a wide range of environments and/or a strong coupling of segmental motions due to electrostatic interaction of ions and that of cations with ether oxygens. Such a broadening of the relaxation mode distribution with increasing f is reflected also in the dielectric spectra (see Figure S1, Supporting Information): for low f = 5% and 11%, well-resolved α and α_2 peaks in ε_{der} can be observed. Nevertheless, the α_2 process becomes much broader, and the α process becomes more like a wing than an independent peak for the f = 22% and 26% samples.

To quantify the electrostatic interaction, we explore the degree of overlapping for polarizability volume V_p defined as polarizability divided by a constant $4\pi\varepsilon_0$ with ε_0 the permittivity of vacuum. This definition enables V_p to specify a volume that an ion pair affects.[22] For ionomers, the polarizability is usually governed by the dipole of ion pairs. The average of the dipole moment of ion pairs can be written as $\langle\mu\rangle = \mu^2E/3kT$,[18] with E being the intensity of a small electric field, enabling us to express Debye's polarizability volume as[22,23]

$$V_p = \frac{\langle\mu\rangle}{4\pi\varepsilon_0 E} = \frac{\mu^2}{12\pi\varepsilon_0 kT} \tag{3}$$

Density functional theory (DFT) calculation at 0 K in vacuum shows that the dipole moment of tetra-*n*-butylphosphonium/Br is μ = 12.32 D (see Figure S3(a) and Supporting Information of ab initio calculation). Inserting this value into eq 3, we estimated V_p = 1.85 nm^3 for the tetra-*n*-butylphosphonium/Br pair at T = −75 °C, a temperature close to T_g of those samples (see Table 1). V_pP_0 provides a simple estimation of the degree of polarizability volume overlap in space, V_pP_0 = 0.21, 0.42, 0.82, and 0.98, for samples having f = 5%, 11%, and 22%, and 26%, respectively, meaning that the samples having f = 22% and 26% are close to a threshold where the polarizability volumes overlap. This overlap seems to enhance cooperative motion of the glassy segments, thereby leading to the entire LVE response described by a single KWW with the extraordinarily low value of β. Another reason that possibly also contributes to the cooperative motion of the segments is the unique chemical structure of our ionomers. In Scheme 1, we see that for the ionomers having $f < 1/3$ each ionic momomer has two nearby nonionic monomers. Then, the phosphonium−Br pair can easily bind the nearby ether oxygens to stabilize the ionic pair. Although ionic pairs may associate to form quadrupoles (2 pair → quadrupole), DFT calculation shows that binding energies referenced to isolated ions are E_{pair} = 341 kJ/mol for pair and $E_{quadrupole}$ = 686 kJ/mol for quadrupole in the gas phase (see the structure in Figure S3(b), Supporting Information) that gives $2E_{pair}/E_{quadrupole} \approx 1$, meaning that the pairs have no strong tendency to form a quadrupole and thus the presence of the EO side chain can effectively stabilize the ionic pair to suppress the formation of the quadrupole or larger aggregates, as confirmed in scattering measurements.[15] The ionic pair and ether oxygen of nearby side chains may associate and move in a cooperative way (see Figure S3(c) and Supporting Information of ab initio calculation) to further broaden the relaxation mode distribution. Meanwhile, the relaxation of bound ether oxygen should also be delayed so that the Rouse to sticky Rouse transition becomes less abrupt, with no rubbery plateau. Nevertheless, the lack of plateau does not mean there is no delay with increasing the ionic association because we can clearly see in Figure 1 that the glassy to terminal relaxation broadens significantly with increasing f, and the delay is simply rather subtle.

One of the main purposes of choosing the bulky phosphonium cation is to lower T_g to improve conductivity, due to the well-known weak interaction of large ions.[23] This strategy seems to work because T_g increases by only 15 K with increasing ionic fraction from 0% to 26%. In general, the proximity to T_g determines the segmental mobility, ionic association lifetime, and conductivity in an orderly way. Understanding the relationship between ionic dissociation and conductivity should ultimately improve the design of high conductivity polyelectrolytes. One convenient way to examine this relationship is to test the Barton, Nakajima, and Namikawa (BNN) equation.[23−27] We modify the BNN equation by assuming dielectric α_2 relaxation and conduction have the same diffusive origin as[23,26,27]

$$\sigma_{DC}/\varepsilon_0 = B\omega_{max}\varepsilon_s \tag{4}$$

where ε_s is the static dielectric constant and B is an intensity factor. In Figure 3b, conduction rate $\sigma_{DC}/\varepsilon_0$ is plotted against $\varepsilon_s\omega_{max}$. It is interesting that the proportionality between $\sigma_{DC}/\varepsilon_0$ and $\varepsilon_s\omega_{max}$ holds well for low f = 5% and 11%, while a slight deviation from this proportionality is observed for higher f = 22% and 26%. The origin of this deviation is still not clear, which may be related to a change of ion aggregation status with T.[23] The small B = 0.3 is consistent with weak ionic interactions and little or no ion aggregation.

In conclusion, we examined the LVE and DRS responses of phosphonium ionomers. It is noted that the LVE and DRS provide independent measures of the same ionic dissociation process, as we previously showed for Na-sulfonate PEO-based ionomers.[16] The characteristic times yielded from these two methods agree quantitatively (Figure 3a). Utilizing the DRS α_2 relaxation time, we successfully predict the rubbery modulus for low f = 5% and 11%. The glassy and rubbery moduli merge into an extremely broad process for high f = 22% and 26% due to an enhanced electrostatic interaction, as quantified by the degree of overlapping of polarizability volumes that signifies ion pairs starting to control the orientation of the neighboring ion pairs.

dx.doi.org/10.1021/mz400476w | ACS Macro Lett. 2013, 2, 970−974

It is interesting that the broad process can be described well with the very simple, yet empirical KWW equation, with the lowest $\beta \sim 0.1$ ever seen for polymeric liquids. The α_2 process is further correlated to DC conductivity, in a way similar to the BNN prediction. Consequently, the ionic segmental relaxation of ionomers plays a central role in dynamics, controlling both the association lifetime for viscoelasticity and the ionic conductivity.

It is well-known that for single-ion conductors the conductive and mechanical performances are usually contradictory; enhancing one usually leads to reduction of the other. This study provides a molecular explanation: conductivity and viscoelastic relaxation are both related directly to the ionic dissociation. Therefore, it would be more applicable to separately improve the conductivity and mechanical performance in the design of a single-ion conductor, via either a structural change like a swollen gel or some morphological variation like microphase separation of a hard phase for mechanical strength and a soft phase for ion conduction.

■ ASSOCIATED CONTENT

Supporting Information

Table S1: VFT fitting parameters; Figure S1: DRS responses; Figure S2: $G(t)$ in time domain (also shown in the TOC graphic); Figure S3: detailed results of ab initio calculations. This material is available free of charge via the Internet at http://pubs.acs.org.

■ AUTHOR INFORMATION

Corresponding Author

*E-mail: rhc@plmsc.psu.edu.

Notes

The authors declare no competing financial interest.

[§]Co-first author.

■ ACKNOWLEDGMENTS

Funding from the Department of Energy, Basic Energy Sciences, under grant BES-DE-FG02-07ER46409 is gratefully acknowledged.

■ REFERENCES

(1) Eisenberg, A.; Kim, J.-S. *Introduction to ionomers*; Wiley: New York, 1998.

(2) Weiss, R. A.; Fitzgerald, J. J.; Kim, D. *Macromolecules* **1991**, *24* (5), 1071−1076.

(3) Weiss, R. A.; Yu, W. C. *Macromolecules* **2007**, *40* (10), 3640−3643.

(4) Weiss, R. A.; Zhao, H. Y. *J. Rheol.* **2009**, *53* (1), 191−213.

(5) Tierney, N. K.; Register, R. A. *Macromolecules* **2003**, *36* (4), 1170−1177.

(6) Tierney, N. K.; Trzaska, S. T.; Register, R. A. *Macromolecules* **2004**, *37* (26), 10205−10207.

(7) Colby, R. H.; Zheng, X.; Rafailovich, M. H.; Sokolov, J.; Peiffer, D. G.; Schwarz, S. A.; Strzhemechny, Y.; Nguyen, D. *Phys. Rev. Lett.* **1998**, *81* (18), 3876−3879.

(8) Tudryn, G. J.; O'Reilly, M. V.; Dou, S. C.; King, D. R.; Winey, K. I.; Runt, J.; Colby, R. H. *Macromolecules* **2012**, *45* (9), 3962−3973.

(9) Tant, M. R.; Wilkes, G. L. *J. Macromol. Sci.-Rev. Macromol. Chem. Phys.* **1988**, *C28* (1), 1−63.

(10) Rubinstein, M.; Semenov, A. N. *Macromolecules* **1998**, *31* (4), 1386−1397.

(11) Charlier, P.; Jerome, R.; Teyssie, P.; Utracki, L. A. *Macromolecules* **1990**, *23* (13), 3313−3321.

(12) Bazuin, C. G.; Eisenberg, A. *J. Polym. Sci., Part A: Polym. Phys.* **1986**, *24* (5), 1121−1135.

(13) Ye, Y. S.; Elabd, Y. A. *Macromolecules* **2011**, *44* (21), 8494−8503.

(14) Ghassemi, H.; Riley, D. J.; Curtis, M.; Bonaplata, E.; McGrath, J. E. *Appl. Organomet. Chem.* **1998**, *12* (10−11), 781−785.

(15) Liang, S.; O'Reilly, M. V.; Choi, U. H.; Shiau, H.; Bartels, J.; Chen, Q.; Runt, J.; Winey, K. I.; Colby, R. H. *Chem. Mater.* **2013**, submitted.

(16) Chen, Q.; Tudryn, G. J.; Colby, R. H. *J. Rheol.* **2013**, *57* (5), 1441−1462.

(17) Wübbenhorst, M.; van Turnhout, J. *J. Non-Cryst. Solids* **2002**, *305* (1-3), 40−49.

(18) Kremer, F.; Schönhals, A. *Broadband dielectric spectroscopy*; Springer: Berlin; New York, 2003.

(19) Barlow, A. J.; Harrison, G.; Lamb, J. *Proc. R. Soc. London, Ser. A* **1964**, *282* (1389), 228−251.

(20) Baxandall, L. G. *Macromolecules* **1989**, *22* (4), 1982−1988.

(21) Leibler, L.; Rubinstein, M.; Colby, R. H. *Macromolecules* **1991**, *24* (16), 4701−4707.

(22) Atkins, P. W.; DePaula, J. *Physical Chemistry*, 7th ed.; W.H. Freeman: New York, 2002.

(23) Choi, U. H.; Mittal, A.; Price, T. L.; Gibson, H. W.; Runt, J.; Colby, R. H. *Macromolecules* **2013**, *46* (3), 1175−1186.

(24) Barton, J. L. *Verres Refract.* **1966**, *20* (5), 328−335.

(25) Nakajima, T. 1971 Annual Report. In *Conference on Electric Insulation and Dielectric Phenomena*; National Academy of Sciences-National Research Council: Washington, DC, 1972; pp 168−176.

(26) Namikawa, H. *J. Non-Cryst. Solids* **1974**, *14* (1), 88−100.

(27) Namikawa, H. *J. Non-Cryst. Solids* **1975**, *18* (2), 173−195.